

# Presenting an extended evaluation framework for building detection algorithms using high spatial resolution images

Iman Khosravi\*, Mehdi Momeni

Department of Surveying Engineering, Faculty of Civil Engineering and Transportation, University of Isfahan, Isfahan, Iran

## Article history:

Received: 02 December 2016, Received in revised form: 22 March 2017, Accepted: 22 April 2017

## ABSTRACT

This paper aims to provide an extended evaluation framework for building detection algorithms using a diverse set of High Spatial Resolution (HSR) images. The HSR images utilized in this paper were chosen from different places and different sensors, and based on several important challenges in an urban area such as building alignment, density, shape, size, color, height, and imaging angle. The classical evaluation metrics such as detection rate, reliability, false positive rate, and overall accuracy only demonstrate the performance evaluation of an algorithm in relation to the buildings and cannot interpret the mentioned challenges. The extended evaluation framework proposed in this paper composed several extended metrics for performance evaluation of building detection algorithms in relation to these challenges in addition to the classical metrics. The paper intends to declare that the success or failure metrics of a building detection algorithm can have more varieties. In fact, a building detection algorithm may be successful at one or several metrics, whilst it may be unsuccessful at the other metrics.

## KEYWORDS

Evaluation  
Accuracy  
Error matrix  
Building detection  
High spatial resolution images

## 1. Introduction

In the last two decades, the detection of buildings from High Spatial Resolution (HSR) images has received much attention for many applications in Earth Observation and Geomatics Engineering (EOGE) such as map updating, urban planning, 3D modeling, disaster management, and change detection. Until now, many building detection algorithms were proposed in the literatures. The performance evaluation of these algorithms is an important task of the studies (Khoshelham et al., 2010). Usually, several famous and common metrics extracted from the error matrix were used for evaluation of the algorithms such as Detection Rate (DR), Reliability (R), False Positive Rate (FPR), and Overall Accuracy (OA). Their meanings and calculation methods can be found in some studies (e.g. Khoshelham et al., 2010 ; Ghanea et al., 2014 ; Khosravi et al., 2014). Up to now, the HSR images used in the building

detection studies were diverse in terms of building alignment, distance between buildings, building density, building shape, building size, building color, and building height. In addition to the challenges mentioned above, the presence and disturbance of shadows and vegetation areas can be observed in the proximities of buildings (see Table 1). All of these challenges do not exist in the images of the previous studies. Furthermore, the classical evaluation metrics, i.e. DR, R, FPR, and OA, only explain the performance evaluation of algorithms in relation to buildings (Khoshelham et al., 2010). Nonetheless, the effect of some challenges is neglected in these metrics. For example, the classical metrics are not able to indicate the evaluation of algorithms in relation to imaging angle or they cannot demonstrate how much the vegetation, shadow or non-building areas can be removed by algorithms. In fact, they cannot point out whether an algorithm is able to

\* Corresponding author

E-mail addresses: iman.khosravi@eng.ui.ac.ir (I. Khosravi); momeni@ui.ac.ir (M. Momeni)

DOI: 10.22059/eoge.2017.63867.1000

eliminate all the vegetation, shadow or non-building areas from image or not. The main objective of this paper is to introduce a diverse set of HSR images based on all the challenges mentioned above (see Table 1) and then, to provide several quantitative metrics for performance evaluation of building detection algorithms in relation to these Challenges. The next sections of the paper are as follows. In Section 2, a diverse set of HSR imagery is introduced and then several evaluation metrics are provided based on them. These metrics and classical metrics establish an extended evaluation framework. In Section 3, the extended framework is applied in order to compare three building detection algorithms. This section indicates that the success or failure metrics of a building detection algorithm can have a wide range and an algorithm may be more successful or unsuccessful than the other algorithms at one or several evaluation metrics. Finally, Section 4 contains the conclusion of the paper.

## 2. Methodology: Extending evaluation framework

### 2.1 A diverse set of HSR images

Twelve regions were chosen from different places and different sensors (see Figures 1). Regions 1-(a), (e), (f), (g),

(h), (i), (k), and (l) were the pan-sharpened QuickBird images (0.6m resolution) and region 1-(j) was the pan-sharpened GeoEye-1 image (0.5m resolution at stereo mode) of the city of Isfahan. Region 1-(d) was the pan-sharpened GeoEye-1 image (at nadir mode) of the city of Tehran and regions 1-(b) and 1-(c) were the pan-sharpened QuickBird images of the city of Ankara. All the images were pre-processed by histogram stretching to enhance. There were many different urban objects such as roads, yards, shadows, vegetation, green spaces, bare land, and the most important feature, i.e. buildings in these images. They can be thus considered as a diverse set of HSR images in terms of "building alignment and distance, density, shape, color and reflectance, the presence of shadow and vegetation, variation of buildings height, and imaging angle". Based on the most prominent property of each region, twelve regions are categorized as follows:

- Regions (a) and (b) have the buildings with regular alignment, where the former has blocks of buildings, while the latter has single buildings. By contrast, region (c) has the buildings with irregular alignment.

Table 1. The challenges used in previous building detection studies

	Building Alignment	Distance Between Buildings	Building Density	Building Shape	Building Size	Building Color	Building Height	Disturbance of Shadows	Disturbance of Vegetation
Benediktsson et al., 2003				✓	✓	✓		✓	
Jin & Davis, 2005				✓	✓	✓			
Hui et al., 2006				✓	✓				
Zhang et al., 2006				✓	✓	✓	✓		✓
Huang et al., 2008				✓	✓		✓		
Hester et al., 2008					✓	✓			✓
Khoshelham et al., 2010	✓			✓			✓		✓
Bouziani et al., 2010				✓	✓	✓	✓		
Dalla Mura et al., 2010				✓				✓	
Taubenbuck et al., 2010	✓		✓	✓	✓		✓		
Myint et al., 2011				✓	✓				
Huang & Zhang, 2011	✓		✓						
Huang & Zhang, 2012	✓		✓						
Aytekin et al., 2012				✓	✓				
Meng et al., 2012				✓	✓				
Salehi et al., 2012					✓	✓			
Huang & Zhang, 2013						✓		✓	
Sebari & He, 2013					✓	✓	✓		
Ghanea et al., 2014					✓	✓	✓		
Khosravi et al., 2014	✓	✓	✓	✓	✓	✓	✓	✓	✓

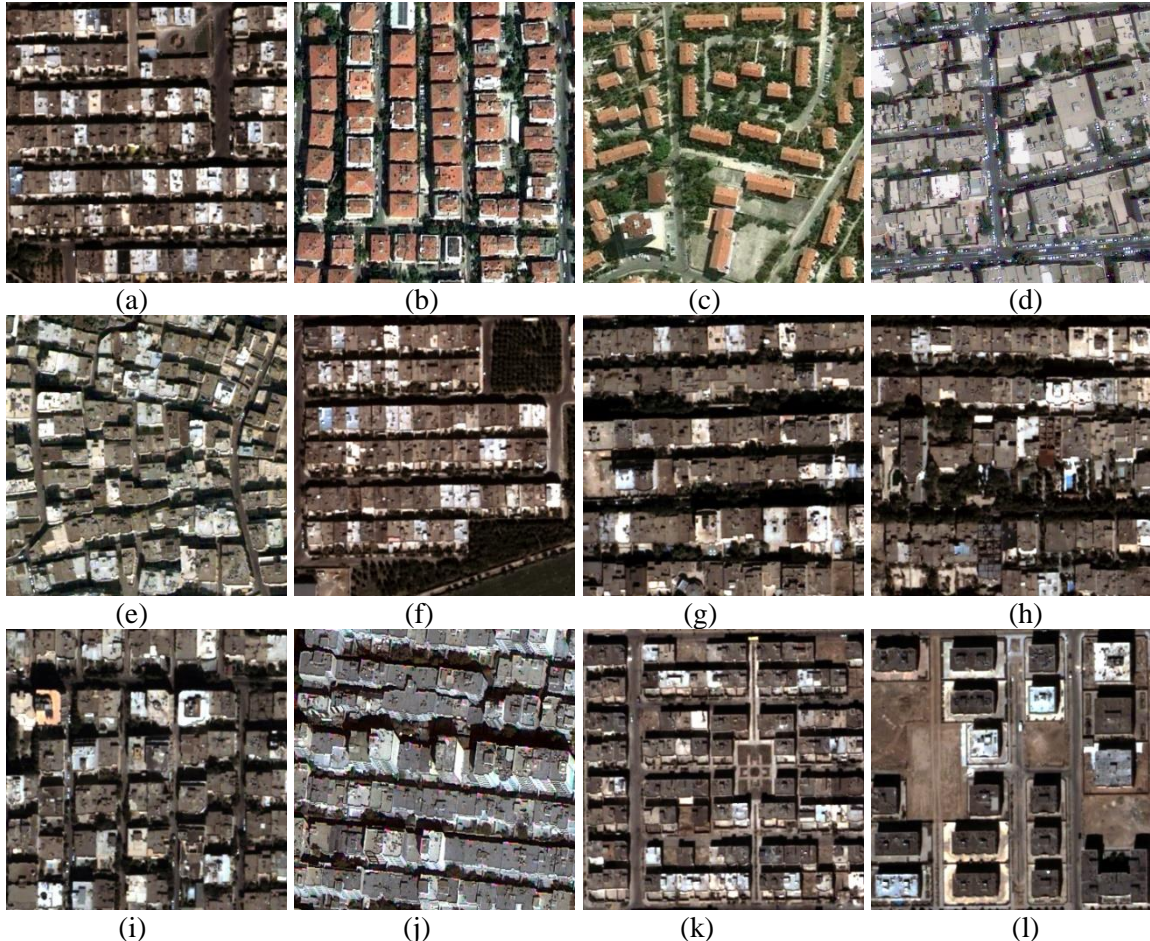


Figure 1. A diverse set of HSR images applied in this paper, (a) Regular blocks, (b) Regular single, (c) Irregular, (d) Positional dense, (e) Ragged edge, (f) Straight edge, (g) Troublesome shadows, (h) Troublesome vegetation, (i) Variation of height, (j) Oblique image, (k) Similar reflectance & blocks, (l) Similar reflectance and single

- The building density of region (d) is relatively high.
- Some buildings of region (e) have the ragged edges, whereas all the buildings of region (f) have straight edges.
- The troublesome urban objects, i.e. shadow and vegetation areas can be observed in proximities of buildings in regions (g) and (h), respectively.
- The buildings of region (i) have diverse height.
- The image of region (j) is an oblique image unlike the other regions.
- Finally, there is similar reflectance (or low contrast) between the building and non-building areas in regions (k) and (l), where the former has blocks of buildings and the latter has single buildings.

## 2.2 Classical evaluation metrics

The classical evaluation metrics such as  $DR$ ,  $R$ ,  $FPR$ , and  $OA$  are defined as follows where the reference data is the buildings image extracted from a digital map ([Khoshelham et al., 2010](#)):

$$DR = \frac{TP}{TP + FN} \quad (1)$$

$$R = \frac{TP}{TP + FP} \quad (2)$$

$$FPR = \frac{FP}{TN + FP} \quad (3)$$

$$OA = \frac{TP + TN}{TP + TN + FP + FN} \quad (4)$$

$TP$  and  $TN$  are the numbers of pixels correctly detected as building and non-building, respectively.  $FP$  is the number of non-building pixels detected as building and  $FN$  is the number of building pixels detected as non-building ([Khosravi et al., 2014](#)).  $FPR$  represents the commission error of buildings produced by algorithm. A higher  $DR$  value indicates the high efficiency of an algorithm in the detection of building. A higher  $R$  and a lower  $FPR$  implies the reliability of the produced results ([Khoshelham et al., 2010](#)).

## 2.3 Extended evaluation metrics

This section aims to provide several quantitative metrics for the evaluation of building detection algorithms based on the applied images:

### 2.3.1 Building alignment

When the building alignment is diverse such as regions (a), (b) and (c), how much building areas can be detected by algorithm. Therefore, Building Detection Rate (*BDR*) index can be a proper metric for performance evaluation of algorithm in relation to building alignment. It is defined by (Khoshelham et al., 2010) as *DR* index Eq. (1) where buildings image extracted from a digital map is considered as the reference data. Thus,  $I_{RB}$ ,  $I_{RS}$  and  $I_{IR}$ , i.e. evaluation metrics, which consider building alignment, are defined as follows:

$$I_{RB} = I_{RS} = I_{IR} = BDR = DR \quad (5)$$

### 2.3.2 Building density

At a dense urban area such as region (d), the amount of building areas can be detected by algorithm. Thus for the performance evaluation of algorithm in relation to building density, again *BDR* index is a good metric, where the reference data is the buildings image extracted from a digital map.  $I_{PD}$ , the evaluation index which considers the building density is defined as follows:

$$I_{PD} = BDR \quad (6)$$

Generally speaking, the *DR* metric can talk about the sensitivity of an algorithm in relation to building alignment and density, in addition to the rate of building regions detected by that algorithm.

### 2.3.3 Building edges

At region (e) or (f), the amount of ragged or straight edges can be detected by algorithm. In these cases, the Ragged Edges Detection Rate (*REDR*) and the Straight Edges Detection Rate (*SEDR*) are defined as follows:

$$REDR = \frac{DRE}{TRE} \quad (7)$$

$$SEDR = \frac{DSE}{TSE} \quad (8)$$

*DRE* and *DSE* are the numbers of detected ragged and straight edges pixels, respectively. *TRE* and *TSE* are the total ragged and straight edges pixels at regions (e) and (f), respectively. Manually ragged edges image of region (e) and manually straight edges image of region (f) are considered as the reference data. Thus, two metrics,  $I_{RE}$  and  $I_{SE}$ , which consider the building edges can be defined as:

$$I_{RE} = REDR \quad (9)$$

$$I_{SE} = SEDR \quad (10)$$

The performance of an algorithm is directly dependent on *REDR* and *SEDR* values.

### 2.3.4 Troublesome objects

Where shadow or vegetation areas are the proximities of buildings such as region (g) or (h), the amount of the shadow or vegetation areas are removed by algorithm. In these cases, the number of shadow and vegetation pixels that have been wrongly detected as buildings are computed in regions (g) and (h), respectively. Thus, the False Shadow Detection Rate (*FSDR*) and the False Vegetation Detection Rate (*FVDR*) are defined as follows:

$$FSDR = \frac{FDS}{TS} \quad (11)$$

$$FVDR = \frac{FDV}{TV} \quad (12)$$

*FDS* and *FDV* are the false number of the detected shadow and vegetation pixels as buildings and *TS* and *TV* are the total shadow and vegetation pixels at regions (g) and (h), respectively. Manually shadow image of region (g) and manually vegetation image of region (h) are considered as the reference data. Two metrics, i.e.  $I_{FS}$  and  $I_{FV}$ , which indicate the ability of an algorithm in eliminating shadow and vegetation areas can be defined as follows:

$$I_{FS} = 1 - FSDR \quad (13)$$

$$I_{FV} = 1 - FVDR \quad (14)$$

In fact, the efficiency and reliability of an algorithm have reverse dependency with the *FSDR* and *FVDR* values.

### 2.3.5 Building height

At an urban area with a variety of buildings heights such as region (i), the more building areas an algorithm is able to detect, the more efficient the algorithm is. Thus, *BDR* index seems to be a proper metric for performance evaluation of algorithm in relation to building height.  $I_{VH}$ , the evaluation index, which considers building height, is defined as follows:

$$I_{VH} = BDR \quad (15)$$

### 2.3.6 Imaging angle

The objective of a 2D building detection algorithm is to detect only roofs, but in an oblique image such as image of region (j), the side view of all or most buildings can be observed in addition to building roofs. In this case, how much the side view areas can be removed by algorithm. Thus, the number of side view pixels that have been wrongly detected as buildings, i.e. False Side View Detection Rate (*FSVDR*) should be computed as follows:

$$FSVDR = \frac{FDSV}{TSV} \quad (16)$$

where,  $FDSV$  is the false number of detected side view pixels as buildings and  $TSV$  is the total side view pixels at region (j). In addition, manually side view image of region (j) is considered as reference data.  $I_{ot}$ , which indicates the ability of algorithm in eliminating the side view areas, is defined as follows:

$$I_{ot} = 1 - FSVDR \quad (17)$$

here, the efficiency and reliability of an algorithm have reverse dependency with the  $FSVDR$  value. A lower  $FSVDR$  implies the high efficiency and reliability of an algorithm in the detection of buildings, whilst its high value indicates the inability of that algorithm in eliminating all side view areas.

### 2.3.7 Similar reflectance

Where there is a similar reflectance between building and non-building areas such as regions (k) and (l), the amount of non-building areas are removed by algorithm. In these cases, the False Non-Building Detection Rate ( $FNBDR$ ), i.e. the number of non-building pixels that have been wrongly detected as buildings, should be computed as follows:

$$FNBDR = \frac{FDNB}{TNB} \quad (18)$$

$FDNB$  is the false number of detected non-building pixels and  $TNB$  is the total non-building pixels at regions (k) and (l). Reference data is the manually non-building image of these regions. Thus,  $I_{SRB}$  (blocks) and  $I_{SRS}$  (single), which indicate the ability of algorithm in eliminating the non-building areas, can be defined as follows:

$$I_{SRB} = I_{SRS} = 1 - FNBDR \quad (19)$$

Similar previous index, the efficiency and reliability of an algorithm have reverse dependency with the  $FNBDR$  value. Consequently, at an urban area with similar reflectance between building and non-building areas, a lower  $FNBDR$  implies the high efficiency and reliability of the algorithm in the detection of buildings and its high value indicates the inability of that algorithm in eliminating all adjacent non-building areas. All the extended metrics mentioned above besides the classical metrics establish an extended evaluation framework. The metrics of this framework and their descriptions are shown in Table 2.

## 3. Experiment and discussion

### 3.1 An overview of three building detection algorithms

For experiment, we selected three recent studies as representatives of all algorithms which had the attractive and complex structures and approximately covered all the processing tricks for building detection using only  $HSR$  images. The first two algorithms are based on the work of (Ghanea et al., 2014 ; Aytekin et al., 2012), where the former is the combination of clustering, and segmentation methods (CS), and the latter is the combination of spectral metrics, clustering, and the morphological methods (ICM). The final algorithm is an Object-Based image Classification (OBC).

#### 3.1.1 Algorithm CS (Clustering and Segmentation)

The algorithm CS presented by (Ghanea et al., 2014) included these steps (Figure 2): in the first step, a k-means clustering ( $K=2$ ) was applied to the original image to convert it to a binary image, consisted of the semi-building layer and the non-building layer. Then a closing morphological operator was used to cover the small non-building areas surrounded by the semi-building layer. Afterwards, a Fuzzy C-Means (FCM) clustering was applied to the semi-building layer to split it into several clusters. Each cluster was decomposed into independent areas using a connected component labelling process. After the FCM clustering, the small pseudo-building areas were eliminated using an area thresholding. The area of the smallest building was considered as the threshold value. Then, a region-growing segmentation was applied to eliminate the large pseudo-building areas. The variance and the area of the segments were used as the similarity criterion for segmenting. The threshold value for area was the area of the largest building. In addition, the variance of all points belonging to each segment at the previous step was considered as the variance threshold for that segment. The holes of the building areas were closed using a filling morphological operator and finally, only the building areas were remained in the image.

#### 3.1.2 Algorithm ICM (Indices, Clustering and Morphological)

The algorithm  $I_{CM}$  was presented by (Aytekin et al., 2012) and had these steps (Figure 3): in step 1, the images of the Normalized Difference Vegetation Index (NDVI) and the shadow index (the ratio of chromaticity to intensity in YIQ color space) were generated. Then, a suitable threshold was determined based on the Otsu's method for each image to eliminate the vegetation and shadow areas, respectively. After masking out the vegetation and shadow areas, the basic image was segmented using a mean-shift method.

Table 2. The developed evaluation framework for building detection algorithms

	<b>Index</b>	<b>Description</b>
<b>Extended Metrics</b>	$I_{RB} = BDR$	Regular Blocks Index
	$I_{RS} = BDR$	Regular Single Index
	$I_{IR} = BDR$	Irregular Index
	$I_{PD} = BDR$	Positional Dense Index
	$I_{RE} = REDR$	Ragged Edge Index
	$I_{SE} = SEDR$	Straight Edge Index
	$I_{FS} = I - FSDR$	False Shadows Index
	$I_{FV} = I - FVDR$	False Vegetation Index
	$I_{VH} = BDR$	Variation of Height Index
	$I_{OI} = I - FSVDR$	Oblique Image Index
	$I_{SRB} = I - FNBDR$	Similar Reflectance Blocks Index
	$I_{SRS} = I - FNBDR$	Similar Reflectance Single Index
<b>Classical Metrics</b>	$I_{DR} = DR$	Detection Rate Index
	$I_R = R$	Reliability Index
	$I_{N-CR} = I - FPR$	Non-Commission Error Index
	$IOA = OA$	Overall Accuracy Index

Thus, man-made areas (include mainly the building rooftops and roads) were extracted after the classification of the vegetation and shadow areas. Afterwards, a modified version of the thinning algorithm (Aytekin et al., 2012) was applied to each segment and then the main roads were separated from other segments using Otsu's thresholding. Next, the small artifacts were filtered using the principle component analysis and a morphological operator such as (Gonzales et al., 2004). Finally, only the building areas were remained in the image.

### 3.1.3 Algorithm OBC (Object-Based Classification)

The most important step in algorithm OBC was segmentation. It used a multiresolution segmentation belonging to eCognition Developer software (eCognition User Guide, 2012). The multiresolution segmentation needed three main parameters to be tuned: scale, shape, and compactness (Baatz & Schape, 2000). After producing the segments, the classes such as roads, vegetation, shadows, bare land, and buildings were defined and the training samples were then collected for each class. Then, the mean values for NDVI, green and brightness, area, length to width ratio, rectangular fit, and shape index were selected as object attributes. Finally, the algorithm determined the label of each segment using the nearest neighbor classifier based on fuzzy logic and then, buildings were separated from the classified image (Figure 4).

## 3.2 Evaluation results

The comparative evaluation results of the three algorithms using the extended framework are shown in Table 3 and also Figure 5. The results are presented in two distinct sections: by the classical metrics and by the

extended metrics.

### 3.2.1 Comparative evaluation by classical metrics

From Table 2, the  $I_{DR}$  rate of algorithm OBC is around 87% which is 10% and 20% higher than the ones of algorithms CS (77%) and ICM (67%), respectively. In addition, the IR rate of algorithm OBC (81%) is 26% and 14% higher as compared to the algorithms CS (55%) and ICM (67%), respectively. Moreover, the commission error of algorithm OBC is around 26% which is 7% lower than the ones of algorithms CS and ICM. In addition, the overall accuracy of algorithm OBC is 20%, which is 12% higher as compared to the two other algorithms. These results can be seen in the right of the vertical dotted line of Figure 5. Therefore, it can be concluded that algorithms-OBC is more efficient and dependable than the algorithms CS and ICM. This issue may be due to the use of segments (instead of single pixels) and also non-spectral features at the object-based process. In comparison between the two non-object-based algorithms, it can be seen that the  $I_{DR}$  rate of algorithm CS is 76% which is around 9% higher than algorithm ICM with the  $I_{DR}$  value of 67%. Conversely, the  $I_R$  value of algorithm ICM (67%) is around 12% higher than the ones of algorithm CS (55%). In addition, the commission error of algorithm ICM (20%) is 19% lower than the ones of algorithm CS (39%). Thus, these results represent that although algorithm CS is more efficient than algorithm ICM in the detection of building, nevertheless algorithm ICM is more dependable than algorithm CS.

### 3.2.2 Comparative evaluation by developed metrics

Although, algorithm OBC was more successful than the other two algorithms at all classical metrics, however it may

be unsuccessful at some developed metrics. In the following, the results of comparative evaluation by developed metrics are provided in detail:

- Building alignment and distance ( $I_{RB}$ ,  $I_{RS}$  and  $I_{IR}$ ):

From Table 2 and Figure 5, algorithm ICM is the most unsuccessful at three metrics  $I_{RB}$ ,  $I_{RS}$  and  $I_{IR}$ . Conversely, algorithm OBC is the most successful at two metrics  $I_{RB}$  (90%) and  $I_{IR}$  (93%); and algorithm CS is the most successful at  $I_{RS}$  (85%) which is 7% higher than the ones of algorithm OBC. These cases indicate "where there are blocks of buildings, algorithm OBC is more successful than the other two algorithms, and algorithm CS is more successful, when there are single buildings while the performance of algorithm ICM is lowest in the two conditions".

- Building positional density ( $I_{PD}$ ):

In the dense urban area, algorithms OBC could be more successful than the other two algorithms with the  $I_{PD}$  rate of 90% versus 80% and 58%. In addition, algorithm CS was more efficient than algorithm ICM in the detection of buildings from a dense area.

- Building Edge ( $I_{RE}$  and  $I_{SE}$ ):

From Table 2, the  $I_{RE}$  and  $I_{SE}$  rates of algorithm OBC are the most (around 100% and 92%), whereas the  $I_{RE}$  of algorithm CS is the lowest (60%) and the  $I_{SE}$  rate of algorithm ICM is the lowest (81%).

- Troublesome Objects ( $I_{FS}$  and  $I_{FV}$ ):

Notable results of Table 2 are related to  $I_{FS}$  and  $I_{FV}$  metrics. As it can be seen, the  $I_{FS}$  and  $I_{FV}$  rates of algorithm ICM have been 100% which are better than the other two algorithms. In

addition, algorithm CS is more successful than algorithm OBC at these two metrics. These two cases indicate that "algorithm ICM is more successful and dependable than the other algorithms (especially object-based method) in eliminating all shadow and vegetation areas from the regions (g) and (h), respectively. Conversely, algorithm OBC is the most unable algorithm in eliminating all shadow and vegetation areas".

- Building Height ( $I_{VH}$ ): Similar to the two previous metrics, the  $I_{VH}$  rate of algorithm ICM is 85% which is better as compared to the other algorithms even object-based method, whereas, the one of algorithm CS is the lowest with the rate of 75%. Thus, "in an urban area with variation of building height, algorithm ICM is the most successful and algorithm CS is the most unsuccessful in the detection of buildings".

- Imaging Angle ( $I_{OI}$ ): The  $I_{OI}$  rate of algorithm OBC is 69% which is much better as compared to the other two algorithms (around 48–51% higher). This case indicates "algorithm OBC is much more successful and dependable than the other two algorithms in eliminating the side view areas of region (j), while algorithm CS has the lowest efficiency".

- Similar Reflectance ( $I_{SRB}$  and  $I_{SRS}$ ): The  $I_{SRB}$  rates of algorithms ICM (82%) and CS (74%) are more than the ones of algorithm OBC (72%). Conversely, the  $I_{SRS}$  rate of algorithms OBC (93%) is much more as compared to the algorithms ICM (74%) and CS (54%).

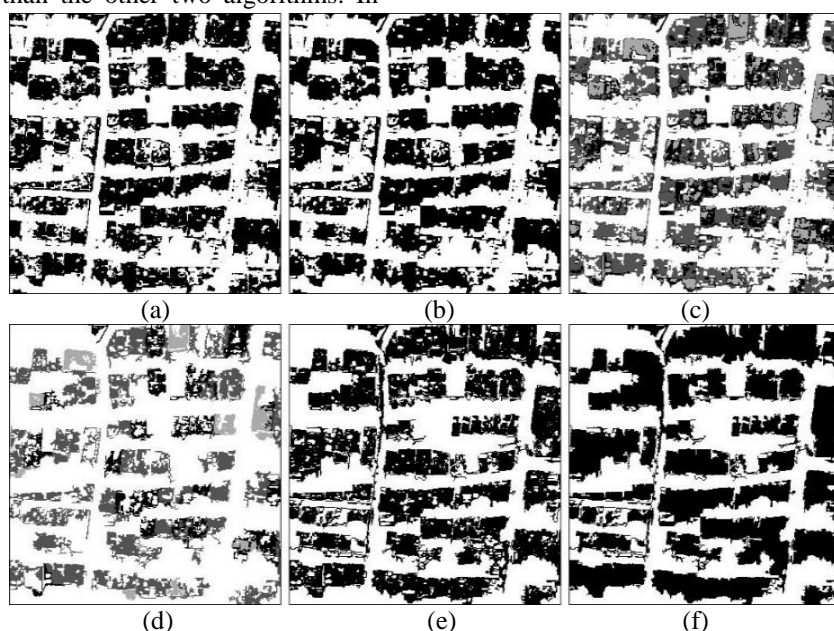


Figure 2. The procedure of algorithm CS, (a) Binary image produced by k-means clustering with  $k = 2$ , (b) Post-processing using a closing morphological operator, (c) Semi-building layer clustering by FCM, (d) Eliminating the small pseudo-building areas, (e) Region-growing method, (f) The final result of building detection

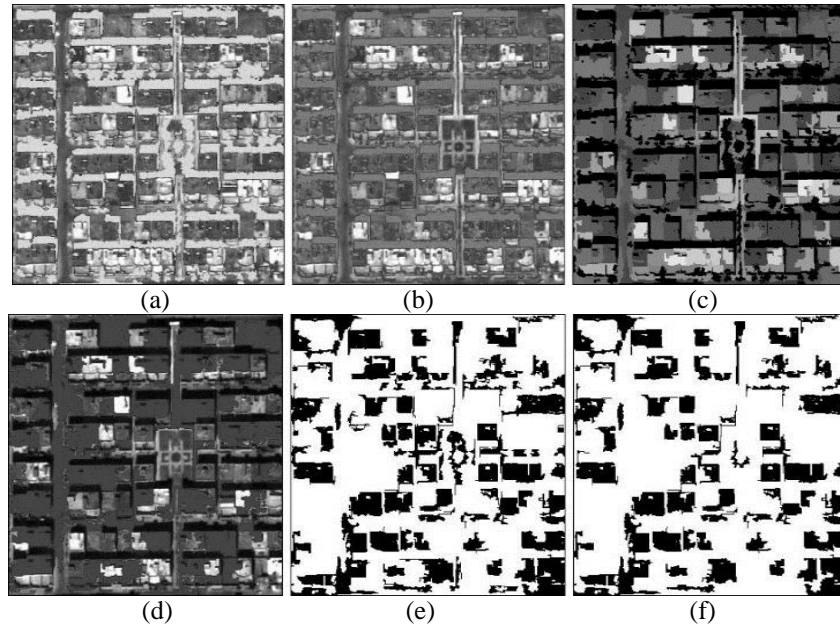


Figure 3. The procedure of algorithm ICM, (a) Masking vegetation, (b) Masking shadows, (c) Man-made image, (d) Masking roads, (e) Filtering the artifacts, (f) The final result of building detection

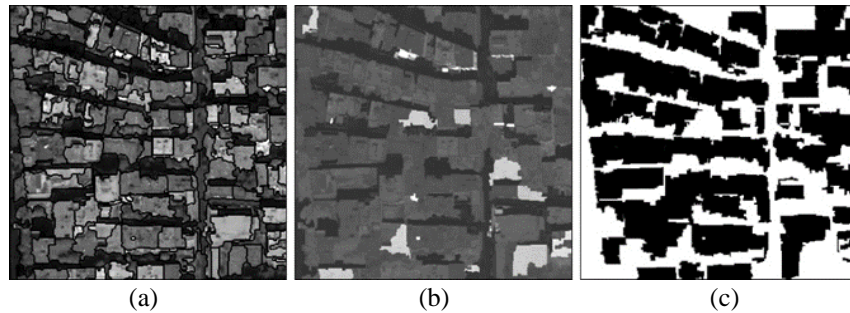


Figure 4. The procedure of algorithm OBC, (a) Multiresolution segmentation, (b) Classified image, (c) The final result of building detection

Table 3. Comparative evaluation results of algorithms using the developed framework

	<b>Index</b>	<b>Algorithm CS</b>	<b>Algorithm ICM</b>	<b>Algorithm OBC</b>
Extended Metrics	$I_{RB}$	81.53	66.56	89.55
	$I_{RS}$	84.73	74.14	77.74
	$I_{IR}$	86.87	67.44	87.11
	$I_{PD}$	79.84	57.50	89.71
	$I_{RE}$	60.04	93.03	99.72
	$I_{SE}$	91.39	80.80	91.53
	$I_{FS}$	98.23	100.00	97.16
	$I_{FV}$	93.63	100.00	84.97
	$I_{VH}$	74.54	84.82	77.47
	$I_{OI}$	18.15	20.79	69.42
	$I_{SRB}$	74.38	81.94	71.88
	$I_{SRS}$	54.27	74.21	93.02
Classical Metrics	$I_{DR}$	76.84	66.54	86.93
	$I_R$	55.13	66.85	80.97
	$I_{N-CR}$	61.25	79.55	87.34
	$IoA$	67.22	74.57	87.19

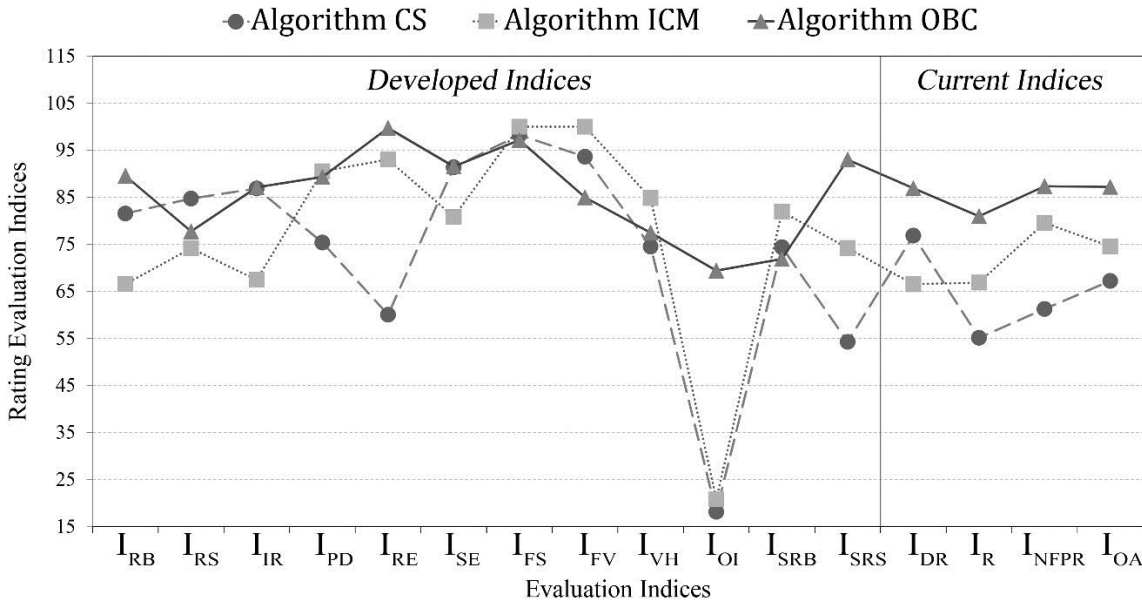


Figure 5. Comparative evaluation using the developed framework between three algorithms

It can be concluded that "algorithms ICM and CS are the most successful in eliminating the non-building areas where there is similar reflectance between the building blocks and non-building areas; while algorithm OBC is the most successful in eliminating the non-building areas, where there is a similar reflectance between single building and non-building areas."

#### 4. Conclusion

This research study which presented an extended evaluation framework indicated that the success or failure metrics of a building detection algorithm can have a wide range. In the proposed framework, the quantitative metrics such as the evaluation metrics in relation to the detection of buildings from a dense urban area, from a region with regular or irregular alignment, from a region with variation of building height, moreover in relation to the eliminating shadow, vegetation, side view and non-building areas were presented. The conclusion of the comparison between the three building detection algorithms using the proposed framework was as follows: Algorithm ICM was more successful than the other two algorithms in eliminating all the troublesome shadow, vegetation and non-building areas (in an urban area with building blocks) and the detection of building areas in a region with variation of height, (i.e. at 4 metrics  $I_{FS}$ ,  $I_{FV}$ ,  $I_{VH}$  and  $I_{SRB}$ ). Moreover, at 6 other metrics ( $I_{RE}$ ,  $I_{OI}$ ,  $I_{SRS}$ ,  $I_R$ ,  $I_{N-CR}$  and  $I_{OA}$ ), it was more successful than algorithm CS. Finally, it was the most unsuccessful at 6 remaining metrics ( $I_{RB}$ ,  $I_{RS}$ ,  $I_{IR}$ ,  $I_{PD}$ ,  $I_{SE}$  and  $I_{DR}$ ). The algorithm OBC was the most successful at 11 metrics ( $I_{RB}$ ,  $I_{IR}$ ,  $I_{PD}$ ,  $I_{RE}$ ,  $I_{SE}$ ,  $I_{OI}$ ,  $I_{SRB}$ ,  $I_{DR}$ ,  $I_R$ ,  $I_{N-CR}$  and  $I_{OA}$ ), it was especially more successful in

eliminating the side view and non-building areas (in an urban area with single buildings). However, at 3 metrics ( $I_{FS}$ ,  $I_{FV}$  and  $I_{SRB}$ ), it was the most unsuccessful. In other words, algorithm OBC was unable to eliminate the troublesome shadow, vegetation areas and non-building areas (at an urban area with building blocks). Finally, it can be concluded that a building detection algorithm may be successful at one or several metrics, while it may fail at the other metrics.

#### References

- Aytekin, Ö., Erener, A., Ulusoy, İ., & Düzgün, S. (2012). Unsupervised building detection in complex urban environments from multispectral satellite imagery. International Journal of Remote Sensing, 33(7), 2152-2177.
- Baatz, M. (2000). Multiresolution segmentation: an optimization approach for high quality multi-scale image segmentation. Angewandte geographische Informationsverarbeitung, 12-23.
- Benediktsson, J. A., Pesaresi, M., & Amason, K. (2003). Classification and feature extraction for remote sensing images from urban areas based on morphological transformations. IEEE Transactions on Geoscience and Remote Sensing, 41(9), 1940-1949.
- Bouziani, M., Goita, K., & He, D. C. (2010). Rule-based classification of a very high resolution image in an urban environment using multispectral segmentation guided by cartographic data. IEEE Transactions on Geoscience and Remote Sensing, 48(8), 3198-3211.
- Dalla Mura, M., Benediktsson, J. A., Waske, B., & Bruzzone, L. (2010). Morphological attribute profiles for the analysis of very high resolution images. IEEE

- Transactions on Geoscience and Remote Sensing, 48(10), 3747-3762.
- eCognition Developer 8.7.2 User Guide. 2012
- Ghanea, M., Moallem, P., & Momeni, M. (2014). Automatic building extraction in dense urban areas through GeoEye multispectral imagery. International journal of remote sensing, 35(13), 5094-5119.
- Gonzalez R.C, Woods R.E, Eddins S.L. Digital Image Processing Using MATLAB, 2nd ed. Prentice-Hall, Inc, 2004.
- Hester, D. B., Cakir, H. I., Nelson, S. A., & Khorram, S. (2008). Per-pixel classification of high spatial resolution satellite imagery for urban land-cover mapping. Photogrammetric Engineering & Remote Sensing, 74(4), 463-471.
- Lu, Y. H., Trinder, J. C., & Kubik, K. (2006). Automatic building detection using the Dempster-Shafer algorithm. Photogrammetric Engineering & Remote Sensing, 72(4), 395-403.
- Huang, X., & Zhang, L. (2011). A multidirectional and multiscale morphological index for automatic building extraction from multispectral GeoEye-1 imagery. Photogrammetric Engineering & Remote Sensing, 77(7), 721-732.
- Huang, X., & Zhang, L. (2013). An SVM ensemble approach combining spectral, structural, and semantic features for the classification of high-resolution remotely sensed imagery. IEEE transactions on geoscience and remote sensing, 51(1), 257-272.
- Huang, X., Zhang, L., & Li, P. (2008). Classification of very high spatial resolution imagery based on the fusion of edge and multispectral information. Photogrammetric Engineering & Remote Sensing, 74(12), 1585-1596.
- Huang X, Zhang L. Morphological building/shadow index for building extraction from high-resolution imagery over urban areas, IEEE Journal of Selected Topics in Applied Earth Observations and Remote Sensing, vol. 5, no. 1, pp. 161–172, February 2012.
- Jin, X., & Davis, C. H. (2005). Automated building extraction from high-resolution satellite imagery in urban areas using structural, contextual, and spectral information. EURASIP Journal on Advances in Signal Processing, 2005(14), 745309.
- Khoshelham, K., Nardinocchi, C., Frontoni, E., Mancini, A., & Zingaretti, P. (2010). Performance evaluation of automated approaches to building detection in multi-source aerial data. ISPRS Journal of Photogrammetry and Remote Sensing, 65(1), 123-133.
- Khosravi, I., Momeni, M., & Rahnemoonfar, M. (2014). Performance evaluation of object-based and pixel-based building detection algorithms from very high spatial resolution imagery. Photogrammetric Engineering & Remote Sensing, 80(6), 519-528.
- Meng, X., Currit, N., Wang, L., & Yang, X. (2012). Detect residential buildings from lidar and aerial photographs through object-oriented land-use classification. Photogrammetric Engineering & Remote Sensing, 78(1), 35-44.
- Myint, S. W., Gober, P., Brazel, A., Grossman-Clarke, S., & Weng, Q. (2011). Per-pixel vs. object-based classification of urban land cover extraction using high spatial resolution imagery. Remote sensing of environment, 115(5), 1145-1161.
- Salehi, B., Zhang, Y., Zhong, M., & Dey, V. (2012). Object-based classification of urban areas using VHR imagery and height points ancillary data. Remote Sensing, 4(8), 2256-2276.
- Sebari, I., & He, D. C. (2013). Automatic fuzzy object-based analysis of VHSR images for urban objects extraction. ISPRS Journal of Photogrammetry and Remote Sensing, 79, 171-184.
- Taubenböck, H., Esch, T., Wurm, M., Roth, A., & Dech, S. (2010). Object-based feature extraction using high spatial resolution satellite data of urban areas. Journal of Spatial Science, 55(1), 117-132.
- Zhang, L., Huang, X., Huang, B., & Li, P. (2006). A pixel shape index coupled with spectral information for classification of high spatial resolution remotely sensed imagery. IEEE Transactions on Geoscience and Remote Sensing, 44(10), 2950-2961.